OTC 21260

Full-Scale Physical Modeling of Pipeline Instability on a Sloping Seabed

F.P. Gao, Institute of Mechanics, CAS; J. Cao, CNOOC Reaserch Center; X.T. Han, Institute of Mechanics, CAS; Y. Sha and E.Y. Zhang, CNOOC Reaserch Center; Y.X. Wu and J.S. Cui, Institute of Mechanics, CAS

Abstract

For the oil and gas exploitation in deep waters, e.g. the continental slopes at South China Sea, the seabed slope would have influence on the pipeline on-bottom stability. In this study, an actuator-driven pipe-soil interaction facility has been specially designed and constructed, for full-scale physical modeling of the current-induced pipeline instability on a sloping sand-bed, including upward instability and downward instability. Based on dimensionless analyses, an ultimate lateral-soil-resistance coefficient is proposed to describe the pipe-soil interaction, and a series of tests have been conducted to reveal the mechanism of pipe instability on a sloping sand-bed. Experimental results indicate that, sand-bed slope angle, pipe's submerged weight and end-constraints have much effect on the pipe stability on a sloping sand-bed.

Introduction

As more and more deepwater oil/gas fileds have been recently found at the continental slope of South China Sea (SCS), the stability of deepwater pipelines on a sloping seabed attracts much attention from the engineering designers and researchers. The seabed in SCS holds rich varieties of its topographic feature including the vast continental shelf, the continental slope and deep sea basin. At the continental slope of SCS, the water depth is generally between 150 to 3,500 meters, and the seabed slope angle changes much at various locations, e.g., the slope angle ranges from 2 to 4 degree at the lower continental slope of northern SCS, and ranges from 3.2 to 7.8 degree at the lower continental slope of southern SCS (Liu *et al.*, 2002). Nevertheless, the influential factor of seabed sloping angle has not been involved in the existing design codes or recommended practices regarding the pipeline on-bottom stability (see, Det Norske Veritas, 2007)

To avoid the occurrence of pipeline on-bottom instability, i.e. the the pipe breakouts from its original site, the seabed must provide enough soil resistance to balance the hydrodynamic loads upon the untrenched pipeline. The pipeline on-bottom stability involves a complex pipe-soil interaction process. Since the 1980s, mechanical actuator experiments have been carried out and some pipe-soil interaction models were proposed to predict pipeline stability induced by the ocean wave in shallow waters (e.g., Wagner *et al.*, 1987; Brenodden, *et al.*, 1989; Zhang, *et al.*, 2002; Teh *et al.*, 2003).

As the oil and gas exploitation moving into deeper waters, ocean current becomes the prevailing hydrodynamic load upon submarine pipelines. For describing the current-induced pipeline lateral stability, Gao *et al.* (2007) conducted a series of flume tests and established an empirical relationship between the dimensionless submerged weight of pipeline and Froude number. Recently, pipe-soil interaction mechanism for steady flow-induced instability of a partially embedded pipeline was further investigated experimentally by employing mechanical actuator to simulate hydrodynamic loads on the pipe (Gao *et al.*, 2011). Nevertheless, the aforementioned studies focused mainly on pipeline on-bottom stability on the horizontal seabed. The effect of seabed slope angle on the pipeline on-bottom stability is far from being well understood.

In this experimental study, the pipeline on-bottom stability on a sloping sandy seabed is investigated with a novel pipe-soil interaction facility, which is capable of modeling the prototype-size pipeline (diameter from 0.2 up to 0.5 m) on an inclined seabed with the slope from 0 to 30 degree. The effects of seabed slope, pipe submered weight and end-constraint on the pipeline on-bottom stability are investigated experimentally.

Full-Scale Modeling of Pipe Instability on a Sloping Seabed

Dimensionless Analyses. The ocean-current induced pipeline on-bottom stability on a sloping sandy seabed involves a complex interaction between flow, pipe and its neighboring soil. The ultimate lateral-soil-resistance (F_{Ru}) for pipe instability is mainly related to the parameters of the pipeline, sand properties and the characteristics of hydrodynamic loads, which can

be expressed in the following non-dimensional forms:

$$\eta_\alpha = f'(\alpha, G, \mu, \frac{\rho_{sat}}{\rho_w}, \frac{D}{d_s}, D_r, \phi, \tan\theta, \frac{e_0}{D}, \lambda, ...)$$ (1)

The detailed dimensionless analyses on the pipeline on-bottom stability on the horizontal sand-bed ($\alpha = 0$) have been made by Gao *et al.* (2011). In Eq. (1), the coefficient of ultimate lateral-soil-resistance (η_α) is defined as the ratio of the ultimate lateral-soil-resistance F_{Ru} ($= F_{Du} - W_S \sin\alpha$) to the corresponding pipe-soil contact force F_{Cu} ($= W_S \cos\alpha - F_{Du}\tan\theta$) perpendicular to the surface of the sloping seabed while the pipe losing lateral stability, i.e.

$$\eta_\alpha = \frac{F_{Ru}}{F_{Cu}} = \frac{F_{Du} - W_S \sin\alpha}{W_S \cos\alpha - F_{Du}\tan\theta}$$ (2)

in which "$F_{Du}\tan\theta$" is the lift force exerted on the pipeline in currents; G is the non-dimensional submerged weight of the pipe:

$$G = \frac{W_S}{\gamma' D^2}$$ (3)

In this study, the influences of the seabed slope angle (α), pipe end-constraint (λ) and submerged weight (G) on the pipe lateral stability are examined intensively. Two types of pipe instability on a sloping seabed have been examined, i.e. (i) Upward Instability: the pipe is moving upward along the sloping seabed (α is positive), and (ii) Downward Instability: the pipe is moving downward (α negative).

Experimental Setup Details. The experimental setup newly constructed at Institute of mechanics, Chinese Academy of Sciences (CAS), was specially designed for simulating the pipe on-bottom stability on a sloping seabed, which is 5.0m long, 1.0m wide and 3.2m high (the height of sand box is 1.5m), as shown in Fig. 1. This facility mainly consists of a test flume with its subsidiary structure, a mechanical-actuator system, and the measurement system, etc. To facilitate the observation of experimental phenomena and data collection, the side-walls of test section are made of toughened glass, and the rests are made of stainless steel plate.
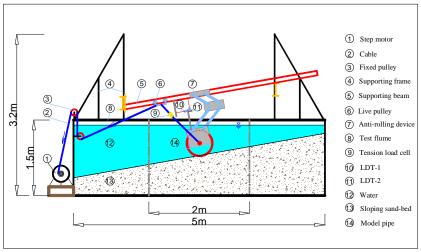

Fig.1 Schematic diagram of the displacement-controlled experimental setup for pipeline stability on a sloping sand-bed.

As well-known, the flow-induced hydrodynamic force on the pipe consists of the drag component (parallel to seabed surface and perpendicular to the pipe axis) and the lift component (perpendicular to seabed surface), which can be evaluated with Morison's equation (Morison *et al.*, 1950), i.e. $F_D = 0.5C_D\rho_w DU^2$, $F_L = 0.5C_L\rho_w DU^2$. Based on the results of the variations of drag (C_D) and lift coefficient (C_L) with the Reynolds number (Re) obtained by Jones (1978), the resultant hydrodynamic load upon the pipe is obliquely upwards with the inclination angle θ ($\approx \arctan(C_L/C_D)$) approximately between 53º~57º. The detailed analyses regarding the hydrodynamic loads on submarine pipeline in currents are given by Gao *et al.* (2011).

To simulate the hydrodynamic force on the pipe in the experiments, the mechanical actuator simulation method has been employed. In the mechanical-actuator system, a displacement-controlled testing program was adopted. A stepper motor was capable of generating an inclined force onto the model pipe via two cables: the front cable with certern length between the pipe and the live pulley, and the other connecting the live pulley and the stepper motor through two fixed pulleys (see Fig.

1). When the position of the supporting beam is given, the angle of the inclined load can be adjusted to a certain value by altering the length of the front cable, on which a tension load cell is installed for measurement of the resultant load from the drag and lift componants.

A saturated sand-bed with certain relative density can be prepared by employing the sand-raining technique. While preparing the sloping sand-bed, a sand-carriage with a slotted bottom, through which the dry sand grains inside can fall into the water, is moving to and fro along the side-walls of the flume by altering its speed to obtain a desired slope angle. As illustrated in Fig. 1, the subsidiary structure consists of supporting frames and a supporting beam laid on them, etc. The rude surface of the sand-bed was then made smooth with a scriper attached onto the supporting beam through a live pulley. In this study, a series of tests have been conducted with the angle of the sand-bed surface in the range of $0^0 \sim 30^0$, to investigate the influence of slope angle on the pipeline stability.

In the synchronous measurement system, two Laser Displacement Transducers (LDT-1 and LDT-2, see Fig. 1) were employed for the noncontact measurement of pipe displacements: LDT-1 is for the measurement of the pipe lateral displacement (parallel to the seabed surface); and LDT-2 for the pipe settlement perpendicular to the seabed. Meanwhile, the tension load cell installed along the front cable is used to measure the exerted inclined load onto the model pipe. The experimental phenomena were being recorded concurrently through the transparent glass wall with a digital video camera.

The testing procedure was adopted as follows: (1) the model pipe was laid downward into the water, and the submerged weight was measured with the tension load cell; (2) while the model pipe touching the sand-bed surface, the two laser displacement transducers (LDT-1 and LDT-2) were triggered to measure the the pipe movements, including the pipe lateral displacement and its initial settlement into the sloping seabed due to its submerged weight; (3) after the initial settlement finished, the stepper motor was started to impose an inclined load onto the pipe for simulating steady current-induced hydrodynamic forces. During the pipe breakout process, the pipe's additional settlement, lateral displacement and the corresponding load were measured simultaneously.

Test pipe with two kinds of end-constraint. For a long-distance submarine pipeline, its on-bottom stability at separate sections is different. The following two end-constraints of the model pipe are taken into account:

End-constraint I: Anti-rolling pipes. Pipe's rolling is restricted, but the pipe may move freely in parallel and perpendicular direction to the seabed surface. An anti-rolling device has been designed, the lower board of which was fixed to the model pipe. The model pipe was attached through the anti-rolling device upward onto the slantwise supporting beam (see Fig. 1).

End-constraint II: Freely-laid pipes. The model pipe may rotate around its axis without end constraint, if the lower board of the anti-rolling device is unlocked to the model pipe.

Three values of the model pipe diameter at full-scale level are adopted in a series of tests, i.e. $D = 0.20, 0.35, 0.50$ m. All of the model pipes are 0.92 m long, with 40 mm gaps to the side walls of the test flume. The values of the pipe's submerged weight vary in the range of $0.55 < G < 1.15$ according to dimensionless analyses (see Eq.(2)), to examine its effects on the pipe on-bottom stability.

Test Sand. A silty fine sand (silica) was adopted to simulate a sandy seabed: the mean grain size $d_{50} = 0.12$ mm, the relative density $D_r = 0.16$ indicating the sand sample is a loose one, the buoyant unit weight of the sand $\gamma' = 9.2 \, \text{kN/m}^3$, the internal friction angle $\phi = 34^0$, the uniformity coefficient $C_u = 3.16$. The coefficient of plexiglass-sand sliding friction $\mu = 0.32$.

Experimental Results and Discussions

Typical features of pipe-soil interaction on a sloping sand-bed. Fig.2 illustrates the development of lateral-soil-resistance (F_R) with the pipe lateral displacement (s/D) for the slope angle $\alpha = \pm 5^0$, 10^0 during pipe losing on-bottom stability. Different from the Case of horizontal seabed (i.e. $\alpha = 0^0$), in the Case of sloping seabed, an initial lateral-soil-resistance is developed while the pipe being laid onto the sloping sand-bed, to balance the component along the seabed surface of the pipe's submerged weight ($W_S \sin \alpha$), so as to keep the pipe stable even without the action of hydrodynamic loads in currents (named as 'static stability').
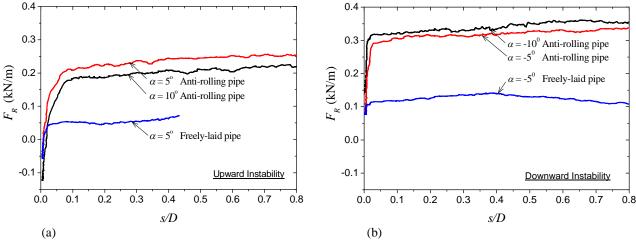
For the Upward Instability (see Fig. 2(a)), with the increase of lateral displacement during the pipe losing lateral stability, the lateral soil resistance (obliquely upward) decreases from certain negative value to zero, and then increases gradually to its maximum value. The ultimate (maximum) soil resistance (F_{Ru}) decreases with the slope angle (α) varying from 5^0 to 10^0. Meanwhile, the additional settlement of the pipe is being gradually developed with increasing pipe lateral displacement (see Fig 3).

For the Downward Instability (see Fig. 2(b)), the lateral soil resistance increases from certain value ($= W_S \sin \alpha$) to its maximum value with increasing lateral displacement, whose direction is always obliquely upward. The ultimate soil-lateral-resistance (F_{Ru}) increases with the slope angle (α) varying from -5^0 to -10^0. The ultimate soil resistances (F_{Ru}) for

Downward Instability (see Fig. 2(b)) are bigger than those for Upward Instability (see Fig. 2(a)).

The effects of pipe end-constraint on the static stability are unignorable. Experimental observation shows that, static instability occured to a freely-laid model pipe while being laid on the sloping sand-bed ($\alpha = 10^0$). Nevertheless, the same model pipe with anti-rolling end-constraint kept stable (see Fig. 2). The ultimate lateral-soil-resistance for the anti-rolling pipe is much larger than that for the freely-laid pipe with a fixed value of pipe submerged weight (W_S).

Fig. 3 shows the variation of pipe's settlement with its lateral displacement while the pipe losing on-bottom stability. In this figure, the negative sign of 'e' means the settlement direction is obliquely downward (normal to the sand-bed surface). As shown in Fig. 3, there exists an initial settlement of the pipe (e_0/D) after being laid onto the seabed surface. For both the anti-rolling pipe and the freely-laid pipe, some additional settlement was further developed while the pipe breaking out from its original site. The additional embedment for the anti-rolling pipe is much larger that that for the freely-laid pipe, indicating the pipe's end-constraint affects significantly its embedment into the soil and further affects the ultimate lateral soil resistance. As shown in Fig. 4, while losing on-bottom stability, the pipe is pushing ahead the neighboring sand particles, especially for the anti-rolling pipes.

(a)   (b)

Fig. 2 The development of lateral soil resistance with increasing lateral displacement while the pipe losing stability on a sloping sand-bed: (a) Upward Instability; (b) Downward Instability. (D = 0.35 m, W_S =0.801 kN/m, G = 0.711, μ = 0.32, d_{50} = 0.12 mm, D_r = 0.16).
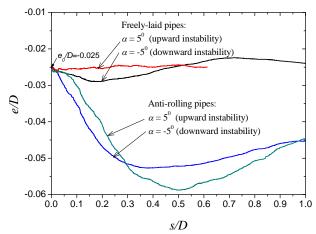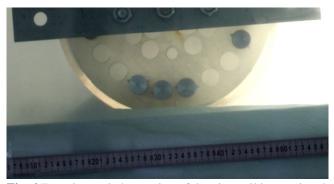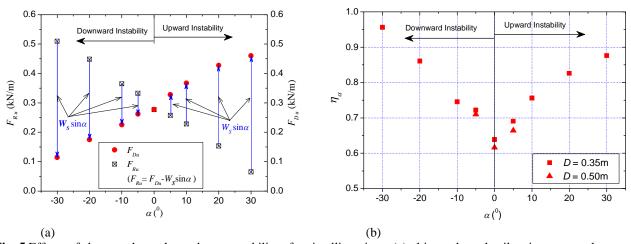

Fig. 3 Additional embedment vs. lateral displacement while pipe losing stability on a sloping sand-bed (D = 0.35 m, W_S =0.801 kN/m, G = 0.711, μ = 0.32, d_{50} = 0.12 mm, D_r = 0.16).

Fig. 4 Experimental observation of the pipe-soil interaction during pipe losing stability on a sloping sand-bed ($\alpha = -5^0$, $D = 0.35$ m, $W_S = 0.801$ kN/m, $G = 0.711$, $\mu = 0.32$, $d_{50} = 0.12$ mm, $D_r = 0.16$).

Effects of slope angle. As aforementioned, the influence of slope angle on the pipeline on-bottom stability is one of the main concerns for the design of submarine pipelines at subsea continental slopes, e.g., at South China Sea. In this study, a series of experiments have been carried out with the newly-designed facility to investigate the effects of slope angle intensively. Fig. 5(a) gives the variations of the ultimate lateral soil resistance (F_{Ru}) and the corresponding ultimate drag force on the anti-rolling pipes induced by currents (F_{Du}) with the slope angle of the sand-bed (α). As indicated in this figure, for a given value of pipe's submerged weight ($W_S = 0.801$ kN/m), with the slope angle increases from -30^0 to 30^0, the ultimate lateral soil resistance decreases, but the corresponding ultimate drag force increases significantly. Note that, $F_{Ru} = F_{Du} - W_S \sin \alpha$. As such, the more precipitous the slope is, the bigger the difference between F_{Ru} and F_{Du} gets. The ultimate value of soil lateral resistance for Downward Instability is larger than that for Upward Instability. Due to the influence of the pipe's submerged self-weight, for the case of Upward Instability, the drag force firstly balances the component of submerged weight ($W_S \sin \alpha$) and then balances the lateral soil resistance (F_{Ru}).

Fig. 5(b) shows the variation of the lateral-soil-resistance coefficient (η_α) with the slope angle (α). No matter for the Upward Instability or Downward Instability, the lateral-soil-resistance coefficient for a sloping sand-bed is larger than that for a horiziontal sand-bed. It is also indicated that, η_α increases with increasing the value of $|\alpha|$, and the value of η_α for Downward Instability is bigger than that for Upward Instability

(a)   (b)
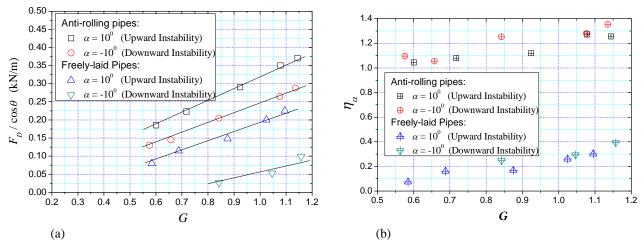
Fig. 5 Effects of slope angle on the on-bottom stability of anti-rolling pipes: (a) ultimate lateral soil resistance vs. slope angle; (b) lateral-soil-resistance coefficient vs. slope angle ($D = 0.35$ m, $W_S = 0.801$ kN/m, $G = 0.711$ [note: $W_S = 1.523$ kN/m, $G=0.662$, for $D = 0.50$ m, see Fig5. (b)], $\mu = 0.32$, $d_{50} = 0.12$ mm, $D_r = 0.16$)

Effects of pipe submerged weight and end-constraint. The effects of non-dimensional submerged weight of the pipe (G) on the ultimate inclined mechanical load ($F_{Du}/\cos\theta$) are shown in Fig.6 (a). For both the anti-rolling pipes and the freely-laid pipes, the ultimate inclined mechanical load increases with increasing the non-dimensional submerged weight. The values of $F_{Du}/\cos\theta$ for Upwad Instability are larger than those for Downward Instability for the same value of G and same

pipe end-constraint.

Fig. 6(b) gives the relationship between the lateral-soil-resistance coefficient and the non-dimensional submerged weight for pipe stability on a sloping sand-bed with a certain slope angle ($|\alpha| = 10^0$). For all the examined cases, the lateral-soil-resistance coefficient (η_α) increases with increasing the non-dimensional submerged weight (G) of the pipes. As indicated in Fig. 6(b), the values of lateral soil resistance coefficient for anti-rolling pipes are much larger than those for the freely-laid pipes. Comapared with the instability directions (i.e. Upward or Downward Instability), the pipe end-constraints have much more effects on the $\eta_\alpha - G$ relationships for pipe stability on a sloping seabed.

| (a) | (b) |

Fig. 6 Effects of non-dimensional submerged weight and end-constraints of the pipeline on the pipe on-bottom stability: (a) ultimate inclined mechanical load vs. non-dimensional submerged weight of the pipe; (b) ultimate lateral-soil-resistance coefficient vs. non-dimensional submerged weight of the pipe (D=0.20 m, $\mu = 0.32$, $d_{50} = 0.12$ mm, $D_r = 0.16$).

Conclusions

The influence of slope angle on the pipeline on-bottom stability is one of the main concerns for the design of submarine pipelines at subsea continental slopes, e.g., at South China Sea. For full-scale simulating pipe on-bottom stability on a sloping seabed, an actuator-driven pipe-soil interaction facility has been specially designed and constructed recently.

According to dimensionless analyses, an ultimate lateral-soil-resistance coefficient (η_α) is proposed to describe the pipe-soil interaction on a sloping sand-bed. A series of tests have been conducted to reveal the mechanism for pipe instability, including Downward Instability and Upward Instability. It is indicated that the sand-bed slope angle, pipe submerged weight and end-constraints have much inflence on pipe on-bottom stability. Typical features of pipe-soil interaction on a sloping sand-bed are summarized, based on the experimental observations. For the case of Upward Instability, due to the action of the submerged weight of the pipe, the current-induced drag force firstly balances the component of submerged weight ($W_S \sin\alpha$) and then balances the lateral soil resistance. No matter for the Upward Instability or Downward Instability, the lateral-soil-resistance coefficient for a sloping sand-bed is larger than that for a horizional sand-bed. It is also indicated that, η_α increases with increasing the value of $|\alpha|$, and the η_α for Downward Instability is bigger than that for Upward Instability.

Acknowledgment

Nomenclature

C_D = drag force coefficient;

C_L = lift force coefficient;

C_u = uniformity coefficient of sand grains;

d_{50} = mean grain size of sand grains;

d_s = sand grain diameter;

D = outer diameter of pipeline;

D_r = relative density of sand;

e = settlement of pipe while losing stability;

e_0 = initial settlement of the pipe;

F_A = applied mechanical load on the pipe;

F_{Cu} = pipe-soil contact force while pipe instability occurs;

F_D = drag force on the pipe;

F_{Du} = ultimate drag force on the pipe;

F_L = lift force on the pipe;

F_R = lateral soil resistance to the pipe (parallel to seabed surface);

F_{Ru} = ultimate lateral soil resistance for pipe instability;

g = gravitational acceleration;

G = non-dimensional submerged weight of the pipe;

s = lateral displacement of the moving pipe;

U = flow velocity of the current;

W_S = submerged weight of the pipe per meter;

α = slope angle of the seabed surface;

ϕ = internal friction angle of soil;

γ' = buoyant unit weight of soil ($\gamma' = \rho_{sat} g - \rho_w g$);

λ = pipe end constraint conditions;

μ = coefficient of sliding friction;

θ = inclination angle of the mechanical loading ($\theta = \arctan\left(F_L / F_D \right)$);

ρ_{sat} = mass density of saturated sand;

ρ_w = mass density of water;

η_α = coefficient of ultimate lateral-soil-resistance for pipe instability on a sloping seabed;

References

1. Brennodden, H., Lieng, J.T., Sotberg, T., and Verley R.L.P., (1989). An energy-based pipe-soil interaction model. Proceeding of 21st Annual Offshore Technology Conference, OTC 6057, pp. 147-158.
2. Det Norske Veritas (2007). On-bottom stability design of submarine pipelines. Recommended Practice, DNV-RP-F109.
3. Gao, F.P., Yan, S.M., Yang, B., and Luo, C.C. (2011). Steady flow-induced instability of a partially embedded pipeline: Pipe-soil interaction mechanism. Ocean Engineering, doi:10.1016/j.oceaneng.2010.09.006
4. Gao, F.P., Yan, S.M., Yang, B., and Wu, Y.X. (2007). Ocean currents induced pipeline lateral stability on sandy seabed. Journal of Engineering Mechanics, ASCE, 133(10): 1086-1092.
5. Jones, W.T. (1978). On-bottom pipeline stability in steady water currents. Journal of Petroleum Technology, 30: 475-484.
6. Liu, Z.S., Zhao, H.T., Fan, S.Q., Chen S.Q. et al. (2002). Geology of South China Sea. Beijing: Scinece Press, China.
7. Morison, J.R., O'Brien, M.P., Johnson, J.W., and Schaaf, S.A. (1950). The forces exerted by surface waves on piles. Petroleum Transactions, AIME, 189: 149-157.
8. Teh, T. C., Palmer, A. C., and Damgaard, J. S. (2003). Experimental study of marine pipelines on unstable and liquefied seabed. Coastal Engineering, 50: 1-17.
9. Wagner, D.A., Muff, J.D., Brennodden, B., and Sveggen, O. (1987). Pipe-soil interaction model. Proceeding of 19th Annual Offshore Technology Conference, OTC5504, pp. 181-190.
10. Zhang, J., Stewart, D.P. and Randolph, M.F. (2002). Modeling of shallowly embedded offshore pipelines in calcareous sand. Journal of Geotechnical and Geoenvironmental Engineering, ASCE, 128: 363-371.